Infrared and Raman Spectra, Vibrational Assignment, Normal Coordinate Analysis, and Barrier to Internal Rotation of *N*-Chloro-*N*-methylmethanamine

J. R. Durig,* N. E. Lindsay,† and T. J. Hizer

Department of Chemistry, University of South Carolina, Columbia, South Carolina 29208
(Received: November 19, 1986; In Final Form: May 15, 1987)

The infrared (3200–80 cm^{-1}) and Raman (3200–10 cm^{-1}) spectra have been recorded of gaseous and solid *N*-chloro-*N*-methylmethanamine (dimethylchloroamine), $(CH_3)_2NCl$, and the corresponding deuterium molecules, $CH_3(CD_3)NCl$ and $(CD_3)_2NCl$. Additionally, the Raman spectra of the liquids have been recorded and qualitative depolarization values have been obtained. A complete vibrational assignment is proposed, based on the infrared band contours, Raman depolarization values, group frequencies, and isotopic shifts. The assignment is supported by a normal coordinate analysis which was carried out by utilizing a modified valence force field to calculate the frequencies and the potential energy distribution. The A′ and A″ methyl torsional fundamentals were observed in the infrared spectrum in the gas phase of the d_0 molecule at 281 and 261 cm^{-1}, respectively, from which the threefold barrier to internal rotation is calculated to be 1658 cm^{-1} (4.74 kcal/mol). From the number of lattice modes observed in the Raman spectrum of the solid, it is concluded that there are at least two molecules per primitive cell. All of these results are compared to similar quantities of some corresponding molecules.

Introduction

For some time we have been interested in the barriers to internal rotation of molecules that have two C_{3v} rotors.[1-6] In several of these studies it has been possible to determine three or more Fourier coefficients of the potential function in two variables and to interpret a great part or all of the features present in the torsional spectra of several two-top molecules. The theoretical background of this method was derived by Groner and Durig[7] and uses the concept of the isometric symmetry group introduced by Bauder et al.[8] One of the earliest studies[9] utilizing this method was the investigation of the torsional spectrum of dimethylamine, where the A″ and A′ fundamentals were observed at 219.4 and 256.3 cm^{-1}, respectively, with four and five "double jumps", respectively, observed for these methyl torsions in the Raman spectrum of the gas. From these data, both the V_{33} (cosine–cosine) and V_{33}' (sine–sine) coupling terms were calculated, and the effective barrier to internal rotation was found to be 1054 cm^{-1} (3.01 kcal/mol), which is 71 cm^{-1} lower than the V_3 calculated from the average of the microwave splittings measured in the first excited state for each torsion.[10] As a continuation of these studies, we have recorded the infrared and Raman spectra of *N*-chloro-*N*-methylmethanamine (dimethylchloroamine), $(CH_3)_2NCl$, and the d_3 and d_6 isotopic species to obtain the frequencies for the methyl torsional modes from which the barriers could be obtained. Additionally, we were interested in comparing the frequencies for the normal modes of these molecules with the corresponding ones for dimethylamine.[11]

There have been very few vibrational studies of molecules that contain nitrogen–chlorine bonds, and there appears to be a large frequency range for the assignment of the N–Cl stretching mode. For example, this mode has been assigned[12,13] at 794 cm^{-1} in $ClNO_2$, but in ClNO it has been placed[14] at 328 cm^{-1}, with the bending mode assigned at 592 cm^{-1}. However, in a more recent vibrational study[15] of this molecule it has been shown that these two modes are extensively mixed but the higher frequency mode may still be as much as 70% of the bend. Therefore, the frequency of the N–Cl stretching vibration in dimethylchloroamine should be of interest for comparison with frequencies for this normal mode in other molecules containing the nitrogen–chlorine bond. Therefore, the results of our vibrational study of $(CH_3)_2NCl$, $CH_3(CD_3)NCl$, and $(CD_3)_2NCl$ are reported herein.

Experimental Section

Dimethylchloroamine was prepared by the reaction of dimethylamine (Matheson) with a 5.25% sodium hypochlorite (Clorox) solution saturated with sodium chloride (Baker Chemical), with dibutyl ether added to facilitate removal of the desired product. The dimethylchloroamine was purified by a trap-to-trap distillation using liquid nitrogen and a liquid nitrogen/*o*-dichlorobenzene slush. Further purification was carried out a low temperature vacuum fractionation column. Dimethyl-d_3- and -d_6-chloroamine were prepared in the same manner from dimethylamine-d_3 and -d_6 (Merck).

Mid-infrared spectra of dimethyl-d_0-, -d_3-, and -d_6-chloroamine were recorded from 3200 to 400 cm^{-1} by using a Digilab Model FTS-14C Fourier transform interferometer equipped with a high-intensity Globar source, a Ge/KBr beam splitter, and a TGS detector. Atmospheric water was removed by purging the interferometer housing with dry nitrogen. Spectra of the gaseous phase were obtained by using a 12-cm cell fitted with CsI windows and a sample pressure of 235 mmHg. The theoretical resolution used was 0.5 cm^{-1}. Spectra of the solids were recorded by using a low-temperature cell equipped with CsI windows as previously described by Baglin et al.[16] The samples were deposited on a CsI substrate held at ~77 K by boiling liquid nitrogen. The samples were annealed until no further changes were observed in the spectra. The theoretical resolution used to obtain the spectra of the solids was 1.0 cm^{-1}.

Far-infrared spectra of the solids were recorded from 600 to 80 cm^{-1} on a Digilab Model FTS-15B Fourier transform interferometer equipped with a high pressure Hg arc lamp, a 6.25-μm Mylar beam splitter, and a TGS detector. The samples were deposited on a wedged silicon substrate encased in a vacuum jacket

† Taken in part from the thesis of N.E.L., which will be submitted to the Department of Chemistry in partial fulfillment of the Ph.D. degree.

(1) Guirgis, G. A.; Durig, J. R.; Li, Y. S. *J. Chem. Phys.* **1985**, *83*, 1507.
(2) Durig, J. R.; Compton, D. A. C.; Rizzolo, J. J.; Jalilian, M. R.; Zozulin, A. J.; Odom, J. D. *J. Mol. Struct.* **1981**, *77*, 195.
(3) Durig, J. R.; Jalilian, M. R.; Sullivan, J. F.; Compton, D. A. C. *J. Chem. Phys.* **1981**, *75*, 4833.
(4) Durig, J. R.; Gerson, D. J. *J. Phys. Chem.* **1981**, *85*, 426.
(5) Durig, J. R.; Gerson, D. J.; Compton, D. A. C. *J. Phys. Chem.* **1980**, *84*, 3554.
(6) Durig, J. R.; Guirgis, G. A.; Compton, D. A. C. *J. Phys. Chem.* **1980**, *84*, 3547.
(7) Groner, P.; Durig, J. R. *J. Chem. Phys.* **1977**, *66*, 1856.
(8) Bauder, A.; Meyer, R.; Gunthard, H. H. *Mol. Phys.* **1974**, *28*, 1305; *Mol. Phys.* **1976**, *31*, 647.
(9) Durig, J. R.; Griffin, M. G.; Groner, P. *J. Phys. Chem.* **1977**, *81*, 554.
(10) Wollrab, J. E.; Laurie, V. W. *J. Chem. Phys.* **1971**, *54*, 532.
(11) Dellepiane, G.; Zerbi, G. *J. Chem. Phys.* **1968**, *48*, 3575.
(12) Ryason, R.; Wilson, M. K. *J. Chem. Phys.* **1954**, *22*, 2000.
(13) Hariharan, T. A. *Proc. Indian Acad. Sci., Sect. A* **1958**, *48A*, 49.
(14) Jones, L. H.; Ryan, R. R.; Asprey, L. B. *J. Chem. Phys.* **1968**, *49*, 581.
(15) McDonald, J. K.; Merritt, J. A.; Kalasinsky, V. F.; Heusel, H. L; Durig, J. R. *J. Mol. Spectrosc.* **1986**, *117*, 69.
(16) Baglin, F. G.; Bush, S. F.; Durig, J. R. *J. Chem. Phys.* **1967**, *47*, 2104.

0022-3654/87/2091-5027$01.50/0

fitted with wedged polyethylene windows. The samples were maintained at ~77 K with boiling liquid nitrogen and annealed until no further changes were observed in the spectra. The spectral resolution used was 1.0 cm^{-1}.

Spectra of the gaseous phase were recorded from 600 to 300 cm^{-1} by using the room temperature vapor pressure in a 12-cm gas cell fitted with CsI windows with a resolution of 0.5 cm^{-1}. Water was removed from the sample by utilizing dried $MgSO_4$ mixed with $^1/_8$-in.-diameter glass beads. The far-infrared spectrum of the vapor phase of $(CH_3)_2NCl$ was also recorded on a Nicolet Model 8000 Fourier transform interferometer equipped with a vacuum bench, a high pressure Hg arc source, and a liquid helium cooled Ge bolometer containing a wedged sapphire filter and polyethylene windows. A 6.25-μm Mylar beam splitter was employed to obtain the spectra from 350 to 80 cm^{-1}. The spectrum was collected at a resolution of 0.12 cm^{-1} by using room temperature vapor pressure in a 20-cm cell fitted with wedged polyethylene windows.

Raman spectra were recorded from 3200 to 50 cm^{-1} (vapor and liquid phases) and from 3200 to 10 cm^{-1} (solid phase) on a Cary Model 82 spectrophotometer equipped with either a Spectra Physics Model 171 argon ion laser operating on the 5145-Å line (liquid d_0 and solid phases) or a Coherent Radiation Model 53 krypton ion laser operating on the 6471-Å line (liquid d_3, liquid d_6, and vapor phases). Obvious decomposition was observed with time for the liquid samples. The spectra of the liquids were obtained by using a glass capillary tube filled under vacuum at room temperature. The laser power at the sample was either 0.5 W (5145-Å line) or 0.4 W (6471-Å line) with a spectral bandwidth of 4 cm^{-1}. Depolarization measurements were made by using the standard Cary accessories. The spectra of the solids were obtained by using a glass capillary tube filled under vacuum inserted in a CTI Cryogenics Model Spectrim cryostat maintained at 100 K. The laser power at the sample was 100 mW with a spectral bandwidth of 2 cm^{-1}. The spectra of the gases were obtained by using a standard Cary multipass accessory. The laser power at the sample was 1.0 W with a spectral bandwidth of 4 cm^{-1}. Reported frequencies are expected to be accurate to at least ±2 cm^{-1} for sharp, resolvable bands.

Vibrational Assignment

N-Chloro-*N*-methylmethanamine-d_0 and -d_6 have C_s point group symmetry, and the 24 fundamental vibrations span the irreducible representations of 13 A′ + 11 A″. All of the fundamentals are active in both the infrared and Raman spectra, with the A″ modes giving rise to depolarized Raman lines. Since the plane of symmetry contains the *a* and *c* axes, the A′ modes will give rise to A, C or A/C hybrid infrared bands in the gas phase whereas the A″ modes will give rise to B-type bands.

Assignments for the normal modes were made by utilizing the Raman depolarization data, isotopic shift data, infrared gas-phase band contours, and group frequencies. In addition, the vibrational assignments (Tables I–III) are supported by normal coordinate calculations.

Carbon–Hydrogen Modes. The CH_3 antisymmetric stretching modes are assigned at 2993 and 2956 cm^{-1} with the A′ and A″ motions contributing to each band. The assignment of the two CH_3 symmetric stretches is not as clear because the overtones and combinations of the CH_3 deformations fall in the region expected for these fundamentals (Figure 1). We have chosen the 2864-cm^{-1} infrared band as one of these fundamentals because of its intensity, but the 2820-cm^{-1} band could be ν_3. The assignment of the out-of-phase CH_3 symmetric stretch at 2898 cm^{-1} must be considered tentative since this band could easily be an overtone or combination of the deformations, and also the separation of ν_3 and ν_{16} seems rather large (Figure 2). For the d_6 molecule the in-phase and out-of-phase modes have all been assigned as being degenerate where the observed splitting in the Raman spectrum of the solid is believed to be due to factor group splitting (Figures 3 and 4). Since the spectroscopic studies[11] on dimethylamine were carried out at low resolution in the carbon–hydrogen stretching region, poor gas-phase contours were obtained and only

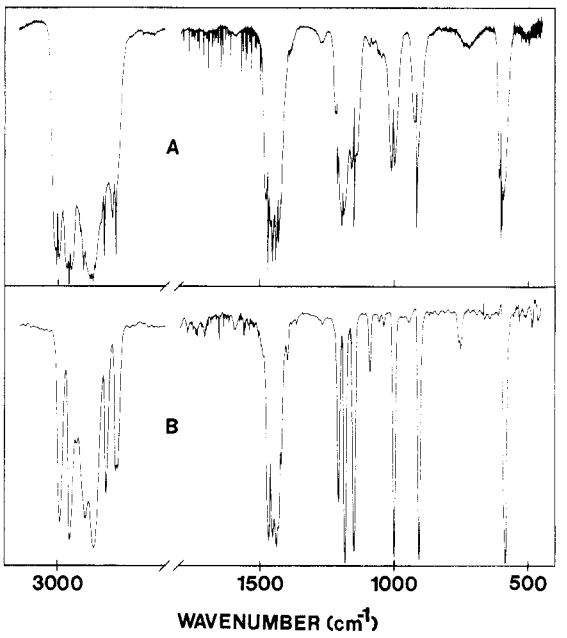

Figure 1. Mid-infrared spectra of gaseous (A) and solid (B) $(CH_3)_2NCl$.

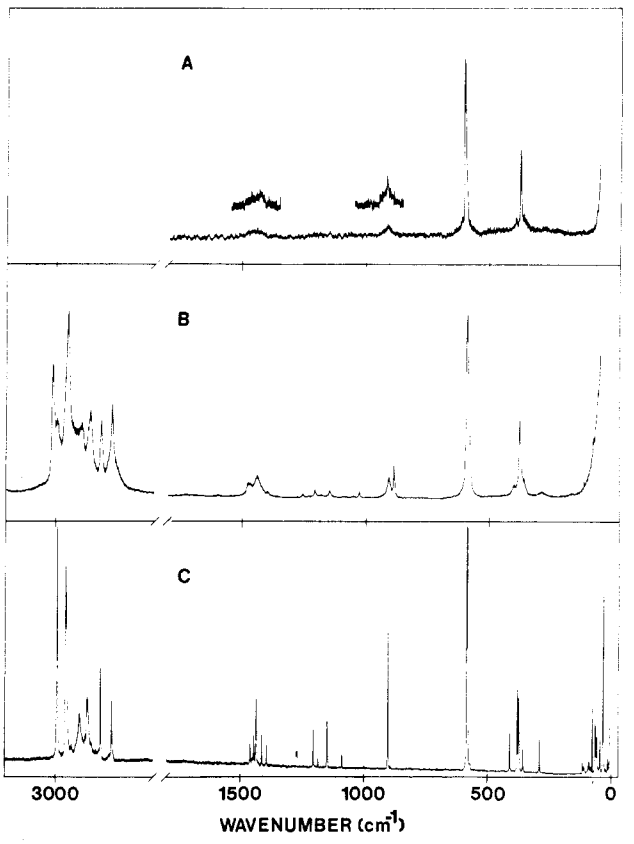

Figure 2. Raman spectra of gaseous (A), liquid (B), and solid (C) $(CH_3)_2NCl$.

limited assignments have been given for the fundamentals of this molecule in this spectral region. However, the d_3 isotopic data (Figures 5 and 6) support the assignments made for the d_0 and d_6 compounds in this spectral region. In the CD_3 stretching region for the d_6 compound there are several relatively weak bands that are obviously overtone or combination bands in Fermi resonance with the fundamentals, but unique assignment for them is not possible.

The two CH_3 symmetric deformations are readily assigned at 1417 and 1399 cm^{-1}. The assignment of the four CH_3 antisymmetric deformations is difficult because there are only two well-defined Raman lines in the expected region, with both being

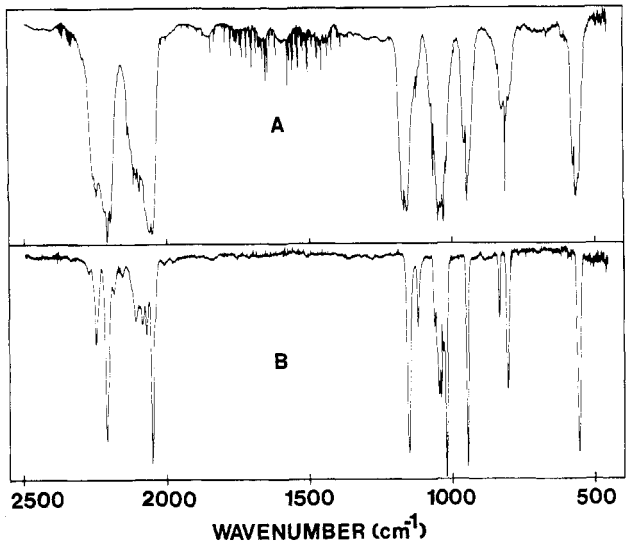

Figure 3. Mid-infrared spectra of gaseous (A) and solid (B) $(CD_3)_2NCl$.

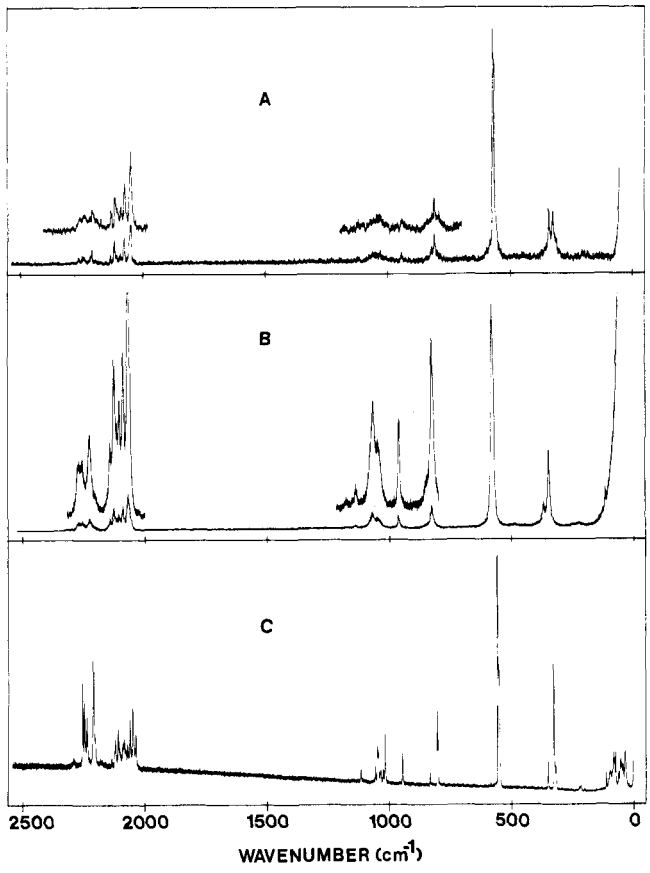

Figure 4. Raman spectra of gaseous (A), liquid (B), and solid (C) $(CD_3)_2NCl$.

depolarized, and the gas-phase infrared band contours are rather nondescript and of little value for assignment purposes. Therefore, we relied on the data from the spectrum of the solid and assumed that the four infrared bands at 1466, 1452, 1438, and 1430 cm^{-1} are due to the CH_3 antisymmetric deformations. Alternatively, the 1430-cm^{-1} band could be due to factor group splitting or arise from an overtone or combination band, in which case any one of the other three bands could be comprised of two fundamentals. Since there is no convenient way of distinguishing between these two possibilities, we have rather arbitrarily chosen the former one. The assignment of the CH_3 rocking modes was straightforward, based on the infrared band contours from the gas phase. The assignment of the CD_3 deformations for the d_6 molecule was rather difficult because of the extensive mixing of several of these modes with the skeletal stretching modes. However, the normal coordinate calculations provide guidance for these assignments.

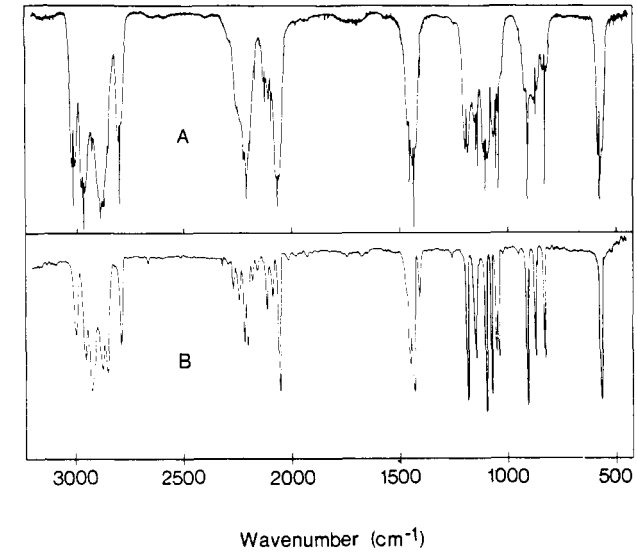

Figure 5. Mid-infrared spectra of gaseous (A) and solid (B) $CH_3(CD_3)NCl$.

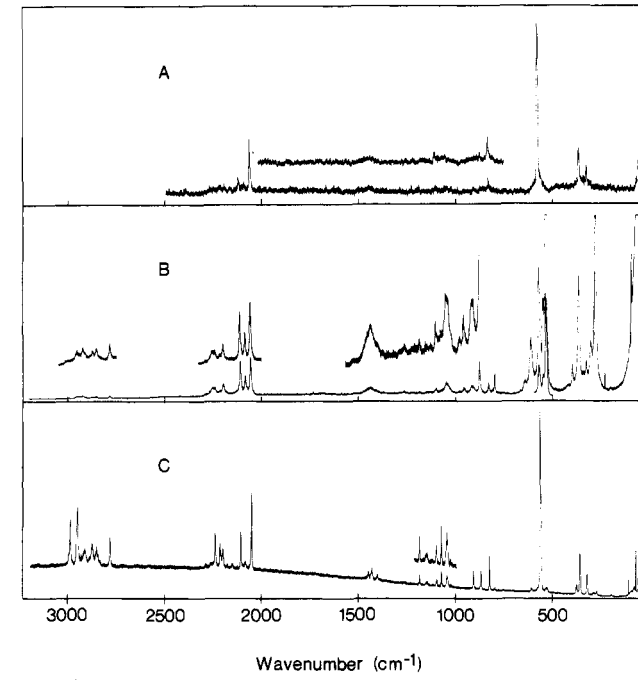

Figure 6. Raman spectra of gaseous (A), liquid (B), and solid (C) $CH_3(CD_3)NCl$.

Skeletal Modes. Dimethylchloroamine has two C–N stretching modes, with the symmetric motion being observed at 920 cm^{-1} in the infrared spectrum of the gas phase. The C–N antisymmetric stretch is observed in the "light" compound at 1008 cm^{-1} and shifts to a higher frequency of 1169 cm^{-1} for the d_6 species and 1154 cm^{-1} for the d_3 species. The corresponding mode in dimethylamine has a similar shift with deuteriation.[11] The NCl stretch for the d_0 compound is assigned to the band at 602 cm^{-1} (596 cm^{-1} for the ^{37}Cl isotope) on the basis of its intensity and the observation of $^{35}Cl/^{37}Cl$ splitting. This mode gives rise to the most intense line in the Raman spectrum with isotopic splitting observed in the spectrum of the solid at 586 and 582 cm^{-1}. The NC_2 symmetric deformation is observed at 405 cm^{-1} whereas the two CNCl bending modes are observed at 379 and 360 cm^{-1} (Figure 7) with the latter one being the A″ mode based on the infrared band contour and the depolarized nature of the Raman line.

Torsional Modes. The two CH_3 torsions for the light compound are extremely weak in the far-infrared spectrum of the gas, but they can be assigned to the bands at 281 cm^{-1} (A/C band) for the in-phase motion and 261 cm^{-1} (B type) for the out-of-phase

TABLE I: Observed and Calculated Infrared and Raman Frequencies, Vibrational Assignment, and Potential Energy Distribution for *N*-Chloro-*N*-methylmethanamine-d_0[a]

infrared				Raman							assignment and PED[b]	
gas	rel int	solid	rel int	gas	rel int	liquid	rel int, depolzn	solid	rel int	calcd	ν_i	approx description[c]
3012 R												
3008 Q, A/C	s					3017	m, p			3005	ν_1	CH_3 antisymmetric stretch (98%)
3005 ctr, B	s	2993	s			2998	m, sh, dp	2991	vs	3004	ν_{14}	CH_3 antisymmetric stretch (98%)
2999 P												
2969 R												
2961 Q, A	s	2956	vs			2954	s, p	2957	s	2961	ν_2	CH_3 antisymmetric stretch (99%)
2951 P										2958	ν_{15}	CH_3 antisymmetric stretch (99%)
2920 max	m	2931	m					2933	mw	2958		$2\nu_4$
2900 min	s	2898	s			2897	m, dp	2901	m	2884	ν_{16}	CH_3 symmetric stretch (98%)
2883 max	s											
2878 max	s											
2870 max	s											
2862 Q	s	2864	vs			2862	m, p	2870	m	2885	ν_3	CH_3 symmetric stretch (98%)
2829 Q	s	2820	s			2819	m, p	2817	m			$\nu_6 + \nu_{18}$
2798 R												
2785 Q	s	2785	s									
		2777	s			2776	m, p	2772	m			$2\nu_6$
1482 R												
1473 Q, A	s	1466	vs			1480	w, bd, dp	1464	mw	1456	ν_4	CH_3 antisymmetric deformation (88%)
1463 P												
1456 max	s	1452	s					1456	w	1453	ν_5	CH_3 antisymmetric deformation (94%)
								1448	mw			
1444 max	s	1438	vs			1443	w, bd, dp	1438	m	1456	ν_{17}	CH_3 antisymmetric deformation (89%); CH_3 symmetric deformation (7%)
1432 max	s	1430	s							1448	ν_{18}	CH_3 antisymmetric deformation (98%)
~1420	m	1419	s			~1420	vw	1417	mw	1407	ν_{19}	CH_3 symmetric deformation (82%); CN antisymmetric stretch (10%); CH_3 antisymmetric deformation (7%)
1399 Q	w	1397	m			~1399	vw	1397	mw	1401	ν_6	CH_3 symmetric deformation (86%); CN symmetric stretch (8%)
1223 R												
1214 Q	m	1207	s	1215	vw	1209	w, p	1208	m	1220	ν_7	CH_3' rock (60%); CN symmetric stretch (17%); CH_3 rock (8%); NC_2 symmetric deformation (8%)
1200 R												
1194 ctr, B	m	1183	vs			1184	vw, dp	1189	w	1193	ν_{20}	CH_3' rock (66%); CN antisymmetric stretch (23%)
1187 P												
1162 R												
1152 Q, A/C	s	1149	vs	1152	w	1148	w, p	1152	m	1162	ν_8	CH_3 rock (77%); CH_3' rock (13%); CNCl bend (6%)
1151 Q												
1142 P												
1103 R												
1093 ctr, B	vw	1089	m					1092	w	1091	ν_{21}	CH_3 rock (85%); CN antisymmetric stretch (13%)
1087 P												
1013 R												
1008 ctr, B	m	999	vs					996	vw	1007	ν_{22}	CN antisymmetric stretch (51%); CH_3' rock (30%); CH_3 rock (16%)
1002 P												
928 R				930	w							
920 Q, A/C	s	905	vs	918	mw	911	mw, dp	906	s	915	ν_{19}	CN symmetric stretch (67%); CH_3' rock (14%); NCl stretch (7%); CH_3 rock (6%)
913 P												
610 R												
602 Q	m	586	vs	602	s	590	s, p	586	vvs	603	ν_{10}	NCl stretch (45%); CNCl bend (29%); CN symmetric stretch (9%); NC_2 symmetric deformation (9%)
599 Q								582	s			
590 P												
403 R												
396 Q, A	s	405	vs	396	w	406	mw, p	412	m	401	ν_{11}	NC_2 symmetric deformation (73%); NCl stretch (13%)
								381	m			
378 Q, A	m	379	s	377	s	378	m, p	376	m	378	ν_{12}	CNCl bend (68%); NCl stretch (29%)
369 P												
357 min		360	m			360	w, dp	358	mw	362	ν_{23}	CNCl bend (96%)
353 P												
281 Q	w	302	m	281	w	292	w, ?	291	w		ν_{13}	CH_3 torsion
261 min	w	294	m								ν_{24}	CH_3 torsion
								109	w			
								90	mw			lattice modes
								83	w			
								64	m			
								58	m			
								47	m			
								33	vs			
								22	w			
								13	mw			

[a] Abbreviations: s, strong; m, medium; w, weak; v, very; ctr, center; sh, shoulder; bd, broad; max, maximum; min, minimum, P, Q, and R refer to the rotational-vibrational branches. Obvious impurity bands are not listed. [b] Contributions of less than 6% are not included. [c] The notation ′ indicates rocking modes parallel to the plane.

TABLE II; Observed and Calculated Infrared and Raman Frequencies, Vibrational Assignment, and Potential Energy Distribution for *N*-Chloro-*N*-methylmethanamine-d_6[a]

infrared				Raman							assignment and PED[b]	
gas	rel int	solid	rel int	gas	rel int	liquid	rel int, depolzn	solid	rel int	calcd	ν_i	approx description[c]
2294	sh, w					2306	m	2295	mw			
		2272	vw									
2260	m			2263	mw	2255	bd, m, p	2258	s			
2252 R								2250	s			
2247 Q	m	2247	m	2246	mw	2240	m, p	2240	m	2247, 2244	ν_1, ν_{14}	CD_3 antisymmetric stretches (97%)
2221 R												
2211 Q, C	s	2211	s	2212	m	2207	m, p	2212	s	2223, 2214	ν_2, ν_{25}	CD_3 antisymmetric stretches (97%)
2200 P								2206	sh, m			
2136	sh, m			2138	m			2140	mw			
				2120	m	2124	m, p	2125	m			
2118 R												
2112 Q	m	2110	m	2110	w	2109	ms, p	2112	m			
2108 P												
2096	m	2086	m	2096	w	2099	m, sh, p	2093	m			
						2088	m, p	2088	m			$2\nu_{18}$
2080	sh, m	2071	m	2081	m	2073	m, p	2082	m			
								2075	mw			$2\nu_6$
2064 R								2064	m			
2058 ctr, B	s	2052	vs	2055	m	2052	m, p	2051	m	2077, 2076	ν_3, ν_{16}	CD_3 symmetric stretches (97%)
2054 P								2040	m			
1173 R												
1169 ctr, B	s	1154	s			1159	w, p			1190	ν_{22}	CN antisymmetric stretch (56%); CD_3 symmetric deformation (36%)
1162 P												
1124 Q	m	1121	m	1125	vw	1121	w, p	1121	mw	1157	ν_6	CD_3 symmetric deformation (45%); CN symmetric stretch (44%)
1075 R												
1068 Q, C	m	1062	m	1068	vw			1063	mw	1097	ν_4	CD_3 antisymmetric deformation (62%); CD_3 symmetric deformation (11%); CD_3' rock (9%); NC_2 symmetric deformation (7%)
1053 Q	s							1053	m			
1049 max	s	1048	s	1050	w, bd	1051	m, dp	1050	m	1064	ν_{17}	CD_3 antisymmetric deformation (91%)
1041 max	s	1041	s					1041	mw	1058	ν_{18}	CD_3 antisymmetric deformation (97%)
1033 max	s	1033	m	1032	vw	1028	m, p	1030	mw	1064	ν_5	CD_3 antisymmetric deformation (95%)
1022 Q	m, sh	1022	vs					1022	m	1001	ν_7	CD_3' rock (27%); CD_3 antisymmetric deformation (32%); CD_3 symmetric deformation (15%); CN symmetric stretch (9%); NC_2 symmetric deformation (6%)
993	w, sh									980	ν_{19}	CD_3 symmetric deformation (48%); CD_3' rock (18%); CN antisymmetric stretch (18%); CD_3 antisymmetric deformation (9%)
956 R												
949 Q, C	m	948	vs	948	w	945	m, p	950	m	933	ν_8	CD_3 rock (65%); CNCl bend (11%)
943 P												CD_3' rock (8%)
840	m	835	s			834	w, ?	837	mw	832	ν_{21}	CD_3 rock (50%); CD_3' rock (36%); CN antisymmetric stretch (8%)
825 R												
813 Q, C	s	807	s	813	w	808	m, ?	809	m	751	ν_9	CN symmetric stretch (33%); CD_3 rock (34%); CD_3 symmetric deformation (17%)
805 ctr, B	m	802	sh			798	w, ?	806	m	784	ν_{20}	CD_3' rock (48%); CD_3 rock (39%); CN antisymmetric stretch (8%)
800 P												
577 R												
569 Q	m	557	m	570	s	558	s, p	558	vvs	534	ν_{10}	NCl stretch (50%); CNCl bend (17%);
565 Q								554	vvs			CD_3' rock (11%); CN symmetric
557 P												stretch (10%); CD_3 rock (7%)
344 Q	m	352	s	344	m	349	m, p	354	m	353	ν_{11}	NC_2 symmetric deformation (55%); NCl stretch (25%); CNCl bend (9%)
328 Q	m	329	s	329	m	329	m, p	330	ms	346	ν_{12}	CNCl bend (56%); NC_2 symmetric deformation (32%); CH_3 rock (7%)
330 R												
324 ctr, B	m	323	s					323	m	328	ν_{23}	CNCl bend (93%)
320 P												
		218	m	206	vvw	227	w, p	226	vw		ν_{13}	CD_3 torsion
								221	vw			
		188	vw			208	w, dp	~206	vw		ν_{24}	CD_3 torsion
		118	vw					99	mw			
								85	m			
								58	m			lattice modes
								48	m			
								39	m			
								23	vw			

[a] For abbreviations used, see Table I. Obvious impurity bands are not listed. [b] Contributions of less than 6% are not included. [c] The notation ′ indicates rocking modes parallel to the plane.

TABLE III: Observed and Calculated Infrared and Raman Frequencies, Vibrational Assignment, and Potential Energy Distribution for *N*-Chloro-*N*-methylmethanamine-d_3[a]

infrared				Raman							assignment and PED[b]	
gas	rel int	solid	rel int	gas	rel int	liquid	rel int, depolzn	solid	rel int	calcd	ν_i	approx description[c]
3013 R								2998	sh			
3007 Q, A/C	s	2996	m			2997	vw	2292	m	3004	ν_1	CH_3 antisymmetric stretch (98%)
3000 P												
2969 R												
2960 Q, A/C	vs	2955	m			2957	vw	2956	ms	2960	ν_2	CH_3 antisymmetric stretch (99%)
2952 P												
2922	s	2927	s			2914	vw	2917	mw			$2\nu_7$
2883 Q, C	vs	2877	m			2878	vw	2879	mw	2884	ν_3	CH_3 symmetric stretch (98%)
2871 P												
2864	s											
2849	m	2853	m			2854	vw	2857	mw			
2800 R												
2794 Q, C	s	2787	m			2786	vw	2786	m			
2788 P												
		2270	m					2270	w			
2259	m					2258	w					
2254	m											
2250 max	m	2242	m			2243	w	2244	m	2245	ν_4	CD_3 antisymmetric stretch (97%)
2225	m											
2222 R		2217	m			2216	w	2219	mw			
2207 Q, C	s	2201	m			2200	w	2205	mw	2218	ν_5	CD_3 antisymmetric stretch (97%)
2193 Q	m	2180	m					2183	w			
2171 Q	m	2158	w			2164	w	2162	w			
2142 Q	w											
2132 R												
2124 Q	m	2114	m	2125	w	2111	m	2112	m			$2\nu_{14}$
2107 P												
2098	m	2087	m	2095	w	2086	m	2091	w, sh			
2073 R												
2065 Q, C	s	2056	s	2065	w	2060	m	2057	s	2077	ν_6	CD_3 symmetric stretch (97%)
2058 P												
1469 R												
1461 Q, C	s	1455	m			1454	w	1457	mw	1456	ν_7	CH_3 antisymmetric deformation (90%); CH_3 symmetric deformation (6%)
1456 P												
1448 R								1444	m, sh			
1442 Q, C	vs	1436	m			1438	w	1438	mw	1450	ν_8	CH_3 antisymmetric deformation (97%)
1430 P												
								1414	w			
1413 Q	m	1409	m			1413	w	1409	mw	1404	ν_9	CH_3 symmetric deformation (84%); CH_3 antisymmetric deformation (6%)
1203 R												
1198 ctr, B	m	1190	s			1192	vvw	1193	mw	1215	ν_{10}	CH_3' rock (47%); CN antisymmetric stretch (15%); CN symmetric stretch (15%); CD_3 symmetric deformation (9%)
1192 P												
1159 R								1159	w			
1154 Q, C	m	1151	m			1159	vvw	1153	w	1155	ν_{11}	CN antisymmetric stretch (32%); CD_3 symmetric deformation (29%); CH_3 rock (18%); CH_3' rock (8%)
1146 Q												
1119 R								1106	w, sh			
1113 Q	s	1104	s	1113	w	1103	w	1104	mw	1130	ν_{12}	CH_3 rock (55%); CH_3' rock (16%); CH_3 symmetric deformation (10%)
1109 Q												
1100 P												
1085 ctr, B	m	1077	s			1079	vvw	1079	mw	1090	ν_{13}	CD_3 antisymmetric deformation (31%); CN symmetric stretch (17%); CD_3 symmetric deformation (16%); CD_3' rock (8%); CN antisymmetric stretch (6%)
1072 P												
1061 Q	s	1054	m			1048	w	1050	mw	1059	ν_{14}	CD_3 antisymmetric deformation (96%)
1048 Q	s	1043	m							1044	ν_{15}	CD_3 antisymmetric deformation (54%); CN antisymmetric stretch (15%); CN symmetric stretch (12%); CD_3' rock (6%)
928 R												
916 Q, C	s	912	s			913	w	916	m	911	ν_{16}	CN symmetric stretch (11%); CD_3 symmetric deformation (20%); CN antisymmetric stretch (19%); CD_3 rock (17%); CD_3' rock (13%); CH_3 rock (9%)
887 R												
879 Q, A	m	874	m			879	m	877	m	854	ν_{17}	CD_3 rock (54%); CD_3' rock (17%)
872 P												
846 R												
836 Q, C	s	831	m	836	m	832	m	833	m	800	ν_{18}	CD_3' rock (37%); CN symmetric stretch (31%) CD_3 rock (11%); CD_3 symmetric deformation (9%)
829 P												
592 R												

TABLE III (Continued)

infrared				Raman							assignment and PED[b]	
							rel int,					
gas	rel int	solid	rel int	gas	rel int	liquid	depolzn	solid	rel int	calcd	ν_i	approx description[c]
584 Q 572 P	s	570	m	585	s	574	s	569	vvs	562	ν_{19}	NCl stretch (46%); CNCl bend (22%); CD_3' rock (9%); CN symmetric stretch (9%); NC_2 symmetric deformation (6%)
		380	m			400	m	386	mw, sh	378	ν_{20}	NC_2 symmetric deformation (48%); NCl stretch (24%); CNCl bend (7%)
								383	mw			
		375	m	369	m	367	s	366	m	368	ν_{21}	CNCl bend (51%); NC_2 symmetric deformation (27%); CNCl bend (12%)
		330	w	329	m	328	m	329	mw	337	ν_{22}	CNCl bend (76%); CNCl bend (13%)
		290	w					282	vw		ν_{23}	CH_3 torsion
						208	vw	204	vw		ν_{24}	CD_3 torsion
								87	w			
								67	m			
								60	m			
								58	m, sh			lattice modes
								46	m			
								34	s			
								14	w			

[a] For abbreviations used, see Table I. Obvious impurity bands are not listed. [b] Contributions of less than 6% are not included. [c] The notation ′ indicates rocking modes parallel to the plane.

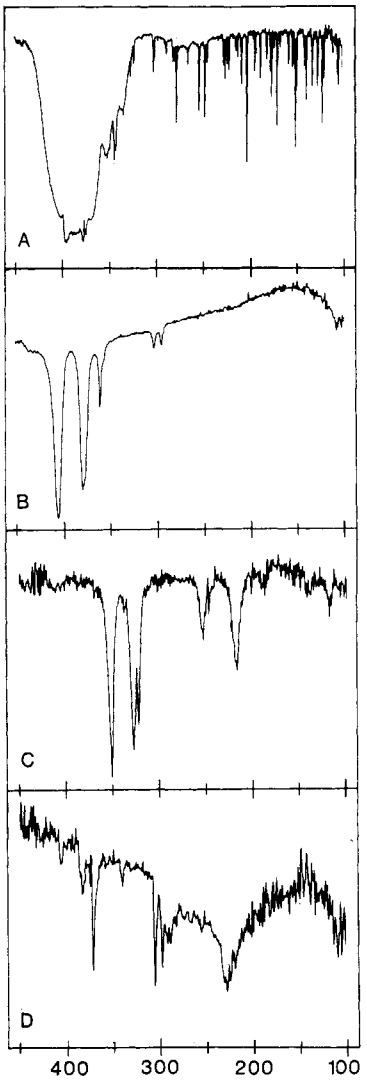

Figure 7. Far-infrared spectra of gaseous d_0 (A), solid d_0 (B), solid d_6 (C), and solid d_3 (D) $(CH_3)_2NCl$.

vibration. In the d_6 compound, the CD_3 torsions were too weak to be observed in the gas phase, so the far-infrared spectrum of the d_3 molecule in the gas phase was not attempted. However, in the spectra of the solids both torsions were observed for both the d_3 and d_6 molecules. The in-phase and out-of-phase torsions for the d_3 compound are observed at ~290 and 204 cm^{-1} in the Raman spectrum of the solid, respectively. In the d_6 compound the torsions are observed at 218 and 188 cm^{-1}, with the higher frequency band assigned to the in-phase mode.

Normal Coordinate Analysis

A normal coordinate analysis was carried out to determine the degree of mixing and to obtain a better description of the normal modes of dimethylchloroamine and its deuteriated analogues. The analysis was carried out according to the Wilson GF matrix method[17] with the perturbation programs developed by Schachtschneider.[18] The *G* matrix was calculated by using structural parameters obtained from a microwave study of $(CH_3)_2NCl$.[19] The symmetry coordinates for the d_0 and d_6 compounds were constructed from 24 internal coordinates and are similar to those previously defined by Durig et al.[20] for $(CH_3)_2PH$. The initial force constants were taken from $(CH_3)_2NH$[11] and ONCl.[15] The modified internal force constants listed in Table IV are for the d_0 compound, and they fit the observed frequencies to 7.1 cm^{-1} (0.5%).

The *G* matrix for the d_3 analogue was modified to account for the point group symmetry change from C_s to C_1. By use of the force field based on the d_0 internal force constants to predict the frequencies expected for the d_6 and d_3 analogues, fits of 19.8 cm^{-1} (2.3%) and 9.5 cm^{-1} (1.0%), respectively, were obtained. The calculated frequencies and normalized potential energy distribution among the symmetry coordinates are listed for the d_0, d_6, and d_3 isotopic species in Tables I, II, and III, respectively.

The CH and CD stretches exhibit virtually no mixing, and for the light compound the CH_3 deformations are relatively pure. However, there is extensive mixing of the CH_3 rocks with both the C–N antisymmetric and symmetric stretches. This mixing becomes even more extensive in the d_3 molecule, where there is now some mixing with the CD_3 deformations. Of course, in the d_6 molecule the mixing is quite extensive for the CD_3 bending modes where the deformations and rocks mix with the C–N stretches. However, the extent of the mixing for the d_6 molecule is not significantly different from that found for the similar modes in the corresponding deuteriated amine.

(17) Wilson, E. B.; Decius, J. C.; Cross, P. C. *Molecular Vibrations*; McGraw-Hill: New York, 1955 (republished by Dover: New York, 1980).
(18) Schachtschneider, J. H. "Vibrational Analysis of Polyatomic Molecules", Parts V and VII, Technical Reports No. 231 and 57; Shell Development Co.: Emeryville, CA, 1964 and 1965.
(19) Durig, J. R.; Chatterjee, K.; Lindsay, N. E.; Groner, P. *J. Am. Chem. Soc.* **1986**, *108*, 6903.
(20) Durig, J. R.; Hudson, S. D.; Jalilian, M. R.; Li, Y. S. *J. Chem. Phys.* **1981**, *74*, 772.

TABLE IV: Internal Force Constants[a] for $(CH_3)_2NCl$

force const	description[b]	value,[c] mdyn/Å
K_a	N–Cl stretch	2.31
K_b	C–N stretch	4.67
K_c	C–H stretch	4.74
H_α	HCH bend	0.588
H_β	NCH bend	0.811
H_γ	CNCl bend	1.40
H_θ	CNC bend	1.31
$F_{a\gamma}$	NCl stretch/CNCl bend	0.278
$F_{b\alpha}$	CN stretch/HCH bend	−0.354
$F_{b\beta}$	CN stretch/NCH bend (nonunique)	−0.199
$F_{b\gamma}$	CN stretch/CNCl bend	0.287
$F_{b\theta}$	CN stretch/CNC bend	0.571
F_{bb}	CN stretch/CN stretch	0.344
F_{cc}	CH stretch/CH stretch	0.107
$F_{\alpha\alpha}$	HCH bend/HCH bend	0.038
$F_{\alpha\beta}$	HCH bend (nonunique)/NCH bend (unique)	0.096
$F_{\alpha\beta}$	HCH bend (nonunique)/NCH bend (unique)	0.066
$F_{\beta\beta'}$	NCH bend (nonunique)/NCH bend (nonunique)	−0.035
$F_{\beta\beta'}$	NCH bend (nonunique)/NCH bend (unique and nonunique)	0.019
$F_{\beta\beta'}$	NCH bend (unique)/NCH bend (nonunique)	0.072
$F_{\gamma\gamma}$	CNCl bend/CNCl bend	0.242
$F_{\gamma\theta}$	CNCl bend/CNC bend	−0.038

[a] Valence force constants. [b] "Unique" refers to the hydrogen atoms that are trans to the lone pair on the nitrogen atom and essentially bisect the opposing CNCl angles whereas "nonunique" refers to the other four hydrogen atoms [b] All bending coordinates are weighted by 1 Å.

In the skeletal bending region the CNCl in-plane bend is extensively mixed with the NCl stretch and, in fact, the band at 602 cm^{-1} is only 45% NCl stretch with a 29% contribution from the CNCl bend in the d_0 molecule. For the corresponding band at 569 cm^{-1} in the d_6 molecule the mixing with the CNCl bend is decreased but there is now mixing with the CD_3 rock. Additionally, the NC_2 deformation at 344 cm^{-1} is now more extensively mixed with the NCl stretch. Similar mixing is observed for the d_3 molecule, but for all three isotopic species it is clear that the band near 600 cm^{-1} is predominately the NCl stretch with significantly less contribution from this motion to the next two lower frequency bands.

Internal Rotation Barrier

The internal Hamiltonian for $(CH_3)_2NCl$ may be set up according to a $C_{3v}(T)$–$C_s(F)$–$C_{3v}(T)$ semirigid model (T = top, F = frame). This Hamiltonian, based on the internal isometric group, as derived by Groner and Durig[7] is

$$H_I = \tfrac{1}{2}(g^{44}p_0^2 + 2g^{45}p_0p_1 + g^{55}p_1^2) + V(\tau_0,\tau_1)$$

with $V(\tau_0,\tau_1)$ in the standard form as

$$V(\tau_0,\tau_1) = \tfrac{1}{2}[V_{30}(1 - \cos 3\tau_0) + V_{60}(1 - \cos 6\tau_0) + V_{03}(1 - \cos 3\tau_1) + V_{06}(1 - \cos 6\tau_1) + V_{33}(\cos 3\tau_0 \cos 3\tau_1 - 1) + V_{33}'(\sin 3\tau_0 \sin 3\tau_1)]$$

The restrictions imposed on this formula for the $C_s(e)$ model are

$$g^{44} = g^{55}, \quad V_{30} = V_{03}, \quad V_{60} = V_{06}$$

The assignment of the 261-cm^{-1} band to the 1,0 ← 0,0 out-of-phase methyl torsional transition is based on the B-type contour of this band in the far-infrared spectrum of the gas (Figure 8). The Q branch observed at 281 cm^{-1} in the far-infrared spectrum of the gas is accordingly assigned to the 0,1 ← 0,0 in-phase methyl torsional transition. A weak band at 281 cm^{-1} in the Raman spectrum of the gas was also observed for this in-phase transition which provides conclusive evidence for the assignment to the A′ mode. The 0,2 ← 0,1 and 0,3 ← 0,2 transitions for the in-phase methyl torsion are assigned at 276 and 269 cm^{-1} in the far-infrared spectrum of the gas, respectively, on the basis of their observed and calculated relative intensities.

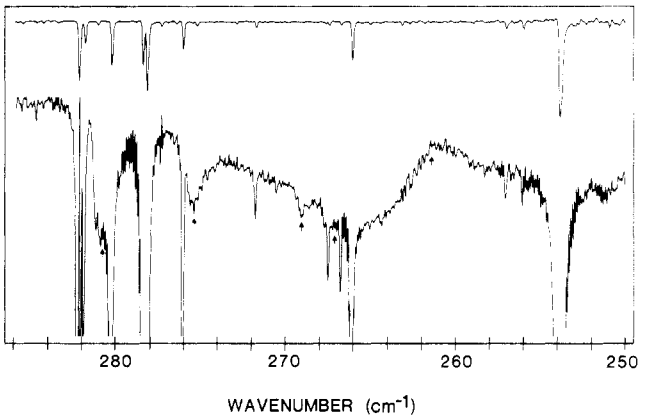

Figure 8. Far-infrared spectrum of gaseous $(CH_3)_2NCl$ where the upper trace is the spectrum of water vapor. The arrows indicate the assignments of the methyl torsional transitions.

TABLE V: Observed Methyl Torsional Data, Assignment, and Torsional Potential Constants (cm^{-1}) for *N*-Chloro-*N*-methylmethanamine

far-infrared, cm^{-1}	assign ($v'v' \leftarrow vv$)	obsd − calcd[a]
281	0,1 ← 0,0	−0.2
267	1,1 ← 1,0	0.2
276	0,2 ← 0,1	−0.2
269	0,3 ← 0,2	0.2
261	1,0 ← 0,0	0.0

parameter	value	dispersion
V_{30}	1783	10
V_{03}	1783	10
V_{33}	125	12
V_{33}'	−129	2
$[(V_{30} + V_{03})/2] - V_{33}$	1658	

[a] Calculated using $g^{44} = g^{55} = 10.7321$, $g^{45} = -0.0439$ cm^{-1}, and the above potential constants.

The threefold barrier to internal rotation was calculated in a series of three steps. The initial calculation utilized the two transitions at 261 and 281 cm^{-1} with only a V_{30} term, which gave an initial barrier of 1666 cm^{-1} (4.77 kcal/mol) with the transitions poorly fit to ±9 cm^{-1}. The next calculation included the transitions at 281, 276, 269, and 261 cm^{-1} with the terms V_{30} = 2159 and V_{33} = 540 cm^{-1}. The barrier was calculated to be 1619 cm^{-1} (4.63 kcal/mol) with a fit of ±9 cm^{-1} for the 0,1 ← 0,0 and 1,0 ← 0,0 transitions and a fit of 2 cm^{-1} for the 0,2 ← 0,1 and 0,3 ← 0,2 transitions. The infrared band at 267 cm^{-1} did not fit the high-frequency series in terms of relative intensity or frequency difference, so it was assigned to the 1,1 ← 1,0 transition. The final calculation included the four previously indicated transitions in addition to this 1,1 ← 1,0 cross term and included V_{30}, V_{33} and V_{33}' terms for an overall fit of ±0.2 cm^{-1} and a threefold barrier to internal rotation of 1658 cm^{-1} (4.74 kcal/mol). The torsional potential constants and the fit to the five observed transitions used in the barrier calculation are summarized in Table V.

Discussion

In order to check the consistency of the proposed vibrational assignment, its agreement with the Teller–Redlich product rule was evaluated. Generally, an agreement of 3–5% between the calculated and observed ratios is sufficient for supporting the validity of the assignment. The calculated ratios for the A′ and A″ symmetry blocks for the $(CH_3)_2NCl$ and $(CD_3)_2NCl$ molecules are 19.65 and 17.48, respectively. The observed ratios are 18.89 and 16.68, respectively, which are 3.9% and 4.6% lower, but it should be noted that the shift factors for the two methyl torsions are not well determined and the frequencies for the normal modes of the A″ symmetry species have errors associated with the determination of the minima for the B-type bands. For the A′ methyl

torsion the Raman line at 206 cm^{-1} for the d_6 molecule has been used in the calculation but the Raman frequency is not known to better than two wavenumbers. Additionally, we used the shift factor of 1.364 for the analogous mode in the A'' symmetry block since this methyl torsion was not observed in the spectrum of the d_6 molecule in the gas phase. Thus, taking these factors into consideration, the agreement between the theoretical and observed ratios appears to be very satisfactory. For the shift ratio for the $(CH_3)_2NCl$ and $CH_3(CD_3)NCl$ molecules, the normal modes are all in the A symmetry block, so that the calculated value is 18.41 and the experimental value is 17.79, which gives an error of 3.4% which again is quite satisfactory. Therefore, the Teller-Redlich product rule supports the proposed vibrational assignment. The assignment of the NCl stretching mode is consistent with the recent work of McDonald et al.[15] on ClNO. As expected, this stretching mode is far from a pure mode where mixing occurs with the CNCl bend, C-N symmetric stretch and NC_2 symmetric deformation. Remarkable consistency was found among the frequencies for the normal vibrations associated with the methyl groups of dimethylamine and those of the corresponding modes of *N*-chloro-*N*-methylmethanamine. It is rather surprising that the heavy chlorine atom with its large electronegativity did not significantly affect the carbon-hydrogen motions of the methyl groups. However, it should be noted that the structural parameters for the common atoms in the $(CH_3)_2NH$ and $(CH_3)_2NCl$ molecules are very similar, including the nitrogen-carbon distances.[19,21]

In $(CH_3)_2NH$ the barrier to internal rotation has been determined[9] to be 1054 cm^{-1} (3.01 kcal/mol); substitution of a chlorine atom for the hydrogen atom increases the barrier to 1658 cm^{-1} (4.74 kcal/mol). This increase of 1.73 kcal/mol is in agreement with the observed increase in the torsional barrier from 679 cm^{-1} (1.94 kcal/mol) in CH_3NH_2[22] to 1323 cm^{-1} (3.78 kcal/mol) in CH_3NHCl.[23] One might expect this additivity to the barriers with substitution to continue with the addition of a second chlorine atom for a hydrogen atom in methylamine. Therefore, one would predict the barrier in CH_3NCl_2 to be around 5.5 kcal/mol. Such substituent additivity has been found for the barriers in the corresponding halocarbons.[24]

The sample of $CH_3(CD_3)NCl$ contained an impurity, which could not be removed, that exhibited interfering vibrations in the Raman spectrum of the liquid. Analysis of the mass spectrum of the $CH_3(CD_3)NCl$ sample indicates that the impurity may be CD_3NCl_2. Many of the observed vibrational bands due to the impurity correlate with the expected vibrational frequencies of CH_3NCl_2[25] upon deuteriation, although it is likely there is an additional impurity that cannot be identified.

There have been few reported[26] force constants for the N-Cl bond. For the ClNO molecule this force constant has been reported[15] to have a value of 1.243 mdyn/Å, which is only about half the value of 2.31 mdyn/Å that we found for this force constant for the $(CH_3)_2NCl$ molecule. However, the N-Cl bond distance[27] in ClNO is 1.973 Å whereas the N-Cl distance[19] in $(CH_3)_2NCl$ is 1.749 Å. The molecule $ClNO_2$ is reported[28] to have an N-Cl bond distance of 1.83 Å with a force constant of 1.840 mdyn/Å. Thus, it appears that the short and presumably stronger N-Cl bond in $(CH_3)_2NCl$ is reflected by the larger force constant, and as the N-Cl bond becomes longer, the force constant value decreases. The force constants for the remaining portion of the molecule appear reasonable compared to those reported[29] from ab initio calculations for methylamine. In the vibrational studies of dimethylamine, the Urey-Bradley force field was utilized, so it is not possible to compare those force constants with the ones obtained in this study. Nevertheless, it appears that a reasonable set of force constants has been obtained for *N*-chloro-*N*-methylmethanamine.

In the Raman spectrum of solid $(CH_3)_2NCl$ there are at least nine observed lattice modes. Unfortunately, they were not nearly as pronounced in the Raman spectrum of either $(CD_3)_2NCl$ or $CH_3(CD_3)NCl$. Therefore, it is not possible to assign the individual transitions to translational or librational modes on the basis of the observed shifts with deuteriation. Nevertheless, the number of lattice modes indicates that there are at least two molecules per primitive cell.

Acknowledgment. We gratefully acknowledge the financial support of this study by the National Science Foundation through Grant CHE-83-11279.

Registry No. $(CH_3)_2NCl$, 1585-74-6; $CH_3(CD_3)NCl$, 109801-36-7; $(CD_3)_2NCl$, 109838-65-5.

(21) Wollrab, J. E.; Laurie, V. W. *J. Chem. Phys.* **1968**, *48*, 5058.
(22) Takagi, K.; Kohma, T. *J. Phys. Soc. Jpn.* **1971**, *30*, 1145.
(23) Caminati, W.; Cervellati, R.; Mirri, A. M. *J. Mol. Spectrosc.* **1974**, *51*, 288.
(24) Durig, J. R.; Guirgis, G. A. *Chem. Phys.* **1979**, *44*, 309.
(25) Haag, W. R. *J. Inorg. Nucl. Chem.* **1980**, *42*, 1123.
(26) Höhne, V. K.; Jander, J.; Knuth, K.; Schlegel, D. *Z. Anorg. Allg. Chem.* **1971**, *386*, 316.
(27) Cazzoli, G.; Degli Esposti, C.; Palmissi, P.; Simeone, S. *J. Mol. Spectrosc.* **1983**, *97*, 165.
(28) Bernitt, D. L.; Miller, R. H.; Hisatsune, I. C. *Spectrochim. Acta, Part A* **1967**, *23A*, 237.
(29) Hamada, Y.; Tanaka, N.; Sugawara, Y.; Hirakawa, A. Y.; Tsuboi, M.; Kato, S.; Morokuma, K. *J. Mol. Spectrosc.* **1982**, *96*, 313.

An Analysis of the Electronic States of Acephenanthrylene

B. F. Plummer

Department of Chemistry, Trinity University, San Antonio, Texas 78284 *(Received: January 7, 1987; In Final Form: April 24, 1987)*

The absorption and emission spectrum of acephenanthrylene is examined experimentally and theoretically by the use of simple perturbational molecular orbital theory and by use of a semiempirical PPP SCF CI calculation. The long-wavelength transition near 440 nm is assigned to a new state called a K-transition that is not present in the precursor analogue phenanthrene. The excited states are found to contain extensive configuration interaction. A weak fluorescence near 540 nm with a quantum yield of 0.0035 is identified as a normal Stokes shifted emission.

Benzo-fused derivatives of acenaphthylene (A) continue to attract study because of their potential carcenogenicity[1,2] and their possible occurrence in the environment.[3] We are interested in learning more about these substances because of their anticipated

0022-3654/87/2091-5035$01.50/0